J Mater Sci (2007) 42:5676–5679
DOI 10.1007/s10853-006-0758-4

Sol–gel synthesis of Ce-substituted $BaFe_{12}O_{19}$

Chang Sun · Kangning Sun

Received: 25 June 2006 / Accepted: 3 August 2006 / Published online: 28 March 2007

Abstract Ce-substituted $BaFe_{12}O_{19}$ ($BaCe_xFe_{12-x}O_{19}$, $x = 0$, 0.01, 0.03, 0.05) was prepared by citrate sol–gel method. The thermal decomposition process of precursor was investigated by TG-DSC. The phase composition of the $BaCe_xFe_{12-x}O_{19}$ was characterized by X-ray powder diffraction analysis (XRD) which reveals that the $BaCe_xFe_{12-x}O_{19}$ crystallizes in a hexagonal structure. The lattice parameter of $BaCe_xFe_{12-x}O_{19}$ increases slightly when Ce was substituted into $BaFe_{12}O_{19}$. The average crystallite size calculated from the XRD line broadening is about 30–33 nm and no intermediate phases are detected in the XRD patterns. The transmission electron microscope (TEM) analysis indicates that the particles of samples obtained are the rod-like morphology.

Introduction

Due to their unique physical properties, Barium hexagonal ferrites ($BaFe_{12}O_{19}$) have been intensively studied as one of the most important hard magnetic materials for high density recording media, permanent magnets, color imaging, and microwave absorbers [1–4]. For example, on the one hand, $BaFe_{12}O_{19}$ presents a high saturation magnetization (M_s = 70 emu g^{-1} at room temperature) and strong uniaxial anisotropy ($K = 16 \times 0.155$ erg g^{-1} at 300°K) [5, 6]; On the other, the planar structure of hexagonal ferrites is the best structure for microwave absorber. It has been predicted that properties such as thermal and electrical conductivity, and magnetic, electrical and optical behavior could be enchanced in materials by substitution with rare earth elements. A large amount of works have been done to modify properties of hexagonal ferrites by substitution Fe^{3+} with rare earth element cation or combination cation, such as La^{3+}, Gd^{3+}, Nd^{3+}, etc. [7, 8]. There are several different synthesis methods used to generate ferrites as reported in the literature including aqueous colloidal precipitation [9], sol–gel method [10], high temperature solid-state [11], and hydrothermal [12]. Sol–gel method has attracted much attention recently because of the well-known inherent advantages of the sol–gel technique to prepare glass, glass–ceramic and ceramics powders. For example, these advantages include: homogeneous molecular mixing, the ability to generate nanosize particles, low processing temperature, and the tremendous flexibility to synthesize nanocrystalline powders, bulk amorphous monolithic solids, and thin films.

In the present work, we focused on synthesis of Ce-substituted $BaFe_{12}O_{19}$ ($BaCe_xFe_{12-x}O_{19}$, $x = 0$, 0.01, 0.03, 0.05) powders by a sol–gel method using stoichiometric amounts of $Ba(NO_3)_2 \cdot 6H_2O$, $Fe(NO_3)_3 \cdot 9H_2O$, $Ce(NO_3)_3 \cdot 6H_2O$, and citric acid as the starting materials. The formation of the $BaCe_xFe_{12-x}O_{19}$ phase, crystalline properties and morphologies of particles have been discussed using X-ray diffraction (XRD) and transmission electron microscopy (TEM).

Experimental

$BaCe_xFe_{12-x}O_{19}$ ($x = 0$, 0,01, 0.03, 0.05) was prepared by sol–gel method. In this paper, all regents used were of

C. Sun (✉)
Key Laboratory of Liquid Structure and Heredity of Materials, Ministry of Education, Shandong University (south part), Jingshi Road 73, Jinan 250061, P. R. China
e-mails: sunchang@mail.sdu.edu.cn; sc7329@163.com

K. Sun
Engineering Ceramics Key Laboratory of Shandong Province, Shandong University (south part), Jingshi Road 73, Jinan 250061, P. R. China

analytical purity and used without further purification. $Ba(NO_3)_2 \cdot 6H_2O$, $Fe(NO_3)_3 \cdot 9H_2O$, and $Ce(NO_3)_3 \cdot 6H_2O$ were used to incorporate metal ions needed.

A stoichiometric amount of $Ba(NO_3)_2 \cdot 6H_2O$, $Fe(NO_3)_3 \cdot 9H_2O$ and $Ce(NO_3)_3 \cdot 6H_2O$ was dissolved in a citric acid aqueous solution under stirring. The molar ratio of nitrates to citric acid was 1:1. After a homogenous transparent solution was achieved within a few minutes, an appropriate amount of ammonia hydroxide solution was added to the solution to adjust the pH value to about 7. During this process, the solution was continuously stirred using a magnetic agitator. After the precursor mixture was heated by water bath at 80 °C and stirring for 3 h, the gel formed. Then the gel was put into drying box at 120 °C, and dried gel was got after 1–2 days. Then the dry gel was milled in a mortar. The dried gel sharply burnt and gave out bright flame when it was calcined at 210 °C in silicon carbide furnace in air so as to remove the organic substance. Finally, they were calcined at 800 °C for 0.5 h, and the $BaCe_xFe_{12-x}O_{19}$ (x = 0, 0.01, 0.03, 0.05) powder was obtained.

The thermal decomposition process of the dried gels was characterized via thermogravimetry (TG, NETZSCH 209) analyses and differential scanning calorimeter (DSC, NETZSCH 404) analyses in a static air atmosphere and with a heating/cooling rate of 20 °C/min. Phase analysis of the synthesized $BaCe_xFe_{12-x}O_{19}$ (x = 0, 0.01, 0.03, 0.05) was conducted using primarily X-ray diffraction using a X-ray powder diffractometer (RIGAKUD/Max-A) using Cu K_α radiation (λ = 1.5405). X-ray powder diffractometer was operated at 60 kV and 40 mA at a 2θ range of 10–80 employing a step size of 0.02 and a speed of 12 deg/min. The microstructure of the synthesized samples was observed by transmission electron microscope (TEM, HITACHI–2500).

Results and discussion

The autocatalytic combustion process of the nitrate–citrate gels was investigated by thermal analysis (TG/DSC) of the dried gel. Figure 1 shows the result of a thermogravimetric analysis combined with differential scanning calorimeter analysis (TG/DSC) conducted on dried gel powder of $BaCe_xFe_{12-x}O_{19}$ (x = 0.03). As expected, the decomposition reaction is strongly exothermic. From DSC data of the $BaCe_xFe_{12-x}O_{19}$ (x = 0.03) dried gel powder the exothermal peak, at 216.3 °C, is relatively sharp and intense. This indicates that the decomposition of the gels occurred suddenly in a single step, as observed in other systems [13]. It has been concluded the exothermic peak in the DSC plot of the as dried gels corresponds to an auto-catalytic anionic oxidation–reduction reaction between the nitrate and citrate

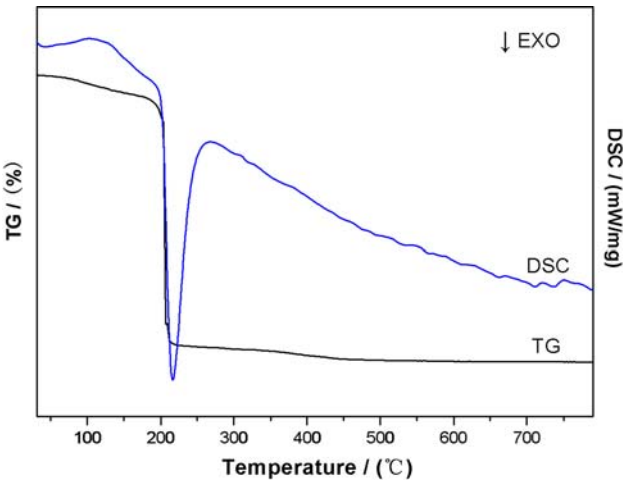

Fig. 1 TG-DSC (differential scanning calorimeter analysis) curves of the nitrate-citrate dried gel

system. From TG data of the dried gel powder of $BaCe_xFe_{12-x}O_{19}$ (x = 0.03), the first sharp weight loss (78.47%), where the exothermal peaks observed (216.3 °C, implied the removal of citric acid and nitrate radical. The second small weight loss 4.6% occurred the range of 228–500 °C. There is no significant weight loss observed above 500 °C, indicating that precursor generates a stable phase after the heat-treatment at temperature above 500 °C.

Phase identification of the as-prepared powder was carried out using XRD patterns. Figure 2 shows the typical XRD patterns of $BaCe_xFe_{12-x}O_{19}$ (x = 0, 0.01, 0.03, 0.05) calcined at 800 °C for 0.5 h in air. All peaks could be indexed to the standard patterns reported the Joint Committee on Powder Diffraction Standards (JCPDS) for hexagonal $BaFe_{12}O_{19}$ (space group P63/mmc (194), file no: PDF#27-1029). No characteristic peaks of intermediate

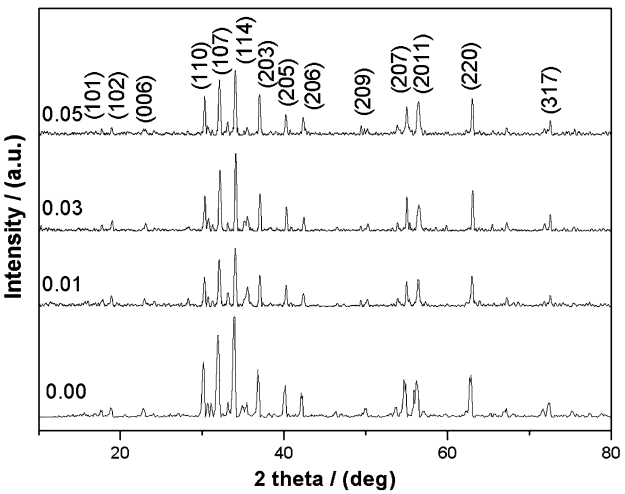

Fig. 2 X-ray diffraction patterns of $BaCe_xFe_{12-x}O_{19}$ (x = 0, x = 0.01, x = 0.03, and x = 0.05)

phases such as barium spinel ferrite ($BaFe_2O_4$), Ce_2O_3, and hematite (α-Fe_2O_3) are detected in the patterns. The Ce can completely substitute into $BaFe_{12}O_{19}$ in the substitution range. For nanocrystalline materials, the size of primary nanoparticles can be estimated by the amount by which the X-ray line is broadened. Figure 3 shows the mean crystallite sizes of $BaCe_xFe_{12-x}O_{19}$ (x = 0.00, 0.01, 0.03, 0.05) calcined at 800 °C for 0.5 h in air, which was calculated from the XRD line broadening of the (114) peak using Scherrer's equation:

$$D_{hkl} = \frac{0.89\lambda}{\beta_i \cos\theta} \tag{1}$$

where λ is the incident wavelength of Cu K_α radiation of the XRD, β_i is the peak width at midheight and θ is the considered angle. The lattice constants a and c are calculated from the value of d_{hkl} corresponding to (008) and (107) peaks according to the following equation:

$$\frac{1}{d_{hkl}^2} = \frac{4}{3}\left(\frac{h^2+k^2+l^2}{a^2}\right) + \frac{l^2}{c^2} \tag{2}$$

in terms of the constants using silicon as an internal standard. The lattice constant of $BaCe_xFe_{12-x}O_{19}$ (x = 0.03) is a = 5.9129 Å and c = 23.2640 Å, which is slightly larger than that of $BaCeFe_{12}O_{19}$ (a = 5.9122 Å and c = 23.2050 Å). These slight changes in the lattice constant may have been caused by the difference between the ionic radius of Ce^{3+}(1.034 Å) and Fe^{3+} (0.645 Å). This reveals that the doping of Ce does not change the hexagonal structure of $BaCeFe_{12}O_{19}$, and Ce was substituted into the crystal lattice.

The typical TEM images of the as-prepared powders of $BaCe_xFe_{12-x}O_{19}$ (x = 0 and 0.03) obtained after heated-treatment at 800 °C for 0.5 h exhibited the rod-like morphology with a length of about 150–200 nm and a diameter of about 30–40 nm showed in Fig. 4. The pictures clearly indicated that most particles are relative straight, and their surfaces are smooth. Most particles formed clusters, because of magnetic interaction between the particles. Thus some nano-rods can be discerned at the clusters.

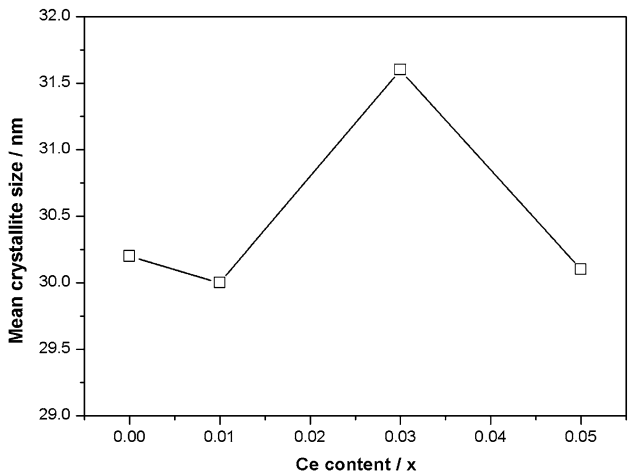

Fig. 3 Average crystallite size of the synthesized powders

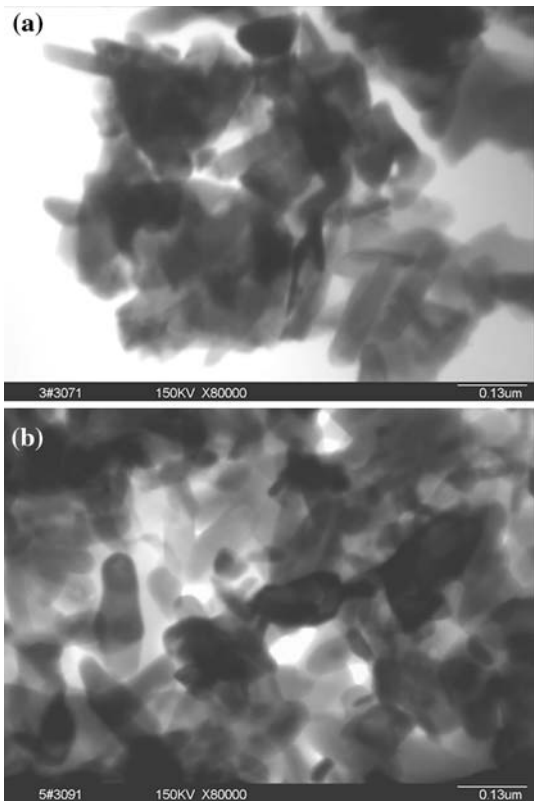

Fig. 4 Transmission electron microscopy (TEM) micrograph of (**a**) $BaFe_{12}O_{19}$ and (**b**) $BaCe_xFe_{12-x}O_{19}$ (x = 0.03)

Conclusion

In summary, we had successfully prepared $BaCe_xFe_{12-x}O_{19}$ (x = 0, 0.01, 0.03, 0.05) by a sol–gel method using stoichiometric amounts of $Ba(NO_3)_2 \cdot 6H_2O$, $Fe(NO_3)_3 \cdot 9H_2O$, and $Ce(NO_3)_3 \cdot 6H_2O$, and citric acid as the starting materials. XRD analysis reveals that the $BaCe_xFe_{12-x}O_{19}$ crystallizes in a hexagonal structure and their average crystallite size is in the range of 30–33 nm. From the TEM observation, the particles of samples exhibited the rod-like morphology.

Acknowledgement This work was supported by the Natural Science Foundation of the People's Republic of China (Grant No. 30540061, 50672051).

References

1. McMichael BD, Shull RD, Swartzendruber LJ, Bennett LH (1992) J Magn Magn Mater 29:111
2. Lisjak D (2003) Informacije Midem – J Microelectron Electron Compon Mater 33:195
3. Capraro S, Le Berre M, Chatelon JP, Joisten H, Mery E, Bayard B, Rousseau JJ, Barbier D (2004) Sens Actuators A Phys 113:382
4. Wane I, Bessaudou A, Cosset F, Celerier A, Girault C, Decossas JL, Vareille JC (2000) J Magn Magn Mater 211:309
5. Braun PB (1958) Philips Res Rep 12:491
6. Wohlforth EP (1982) Ferromagnetic materials. North-Holland, Amsterdam
7. Guo RQ, Chen YJ, Gu MY, Li HG, Sun PM, Jin YP, Liang L (2003) J Rare Earth 21:543
8. Gu YY, Tan XP, Liang SQ, Sang SB (2004) J Central South Univ Technol 11:166
9. Janasi SR, Rodrigues D, Landgraf FJG, Emura M (2001) Key Eng Mat 189–191:661
10. Mali A, Ataie A (2005) Scripta Mater 53:1065
11. Bera S, Prince AAM, Velmurugan S, Raghavan PS, Gopalan R, Panneerselvam G, Narasimhan SV (2001) J Mater Sci 36:5379
12. Wang JF, Ponton CB, Harris IR (2006) J Magn Magn Mater 298:122
13. Yue ZX, Zhou J, Li LT, Zhang HG, Gui ZL (2000) J Magn Magn Mater 208:55